THE JOURNAL OF BIOLOGICAL CHEMISTRY VOL. 287, NO. 9, pp. 6503–6517, February 24, 2012
© 2012 by The American Society for Biochemistry and Molecular Biology, Inc. Published in the U.S.A.

Cytosolic Carboxypeptidase 1 Is Involved in Processing α- and β-Tubulin*[S]

Received for publication, September 29, 2011, and in revised form, December 8, 2011 Published, JBC Papers in Press, December 14, 2011, DOI 10.1074/jbc.M111.309138

Iryna Berezniuk[‡], Hang T. Vu[§], Peter J. Lyons[¶], Juan J. Sironi[¶‖], Hui Xiao[**], Berta Burd[**], Mitsutoshi Setou[§], Ruth H. Angeletti[**], Koji Ikegami[§1], and Lloyd D. Fricker[‡¶2]

From the Departments of [‡]Neuroscience, [¶]Molecular Pharmacology, and [‖]Pathology, Albert Einstein College of Medicine, Bronx, New York 10461, the [§]Department of Cell Biology and Anatomy, Hamamatsu University School of Medicine, 1-20-1 Handayama, Hamamatsu 431-3192, Japan, and the [**]Laboratory of Macromolecular Analysis and Proteomics, Albert Einstein College of Medicine, Bronx, New York 10461

Background: Several cellular functions for cytosolic carboxypeptidase 1 (CCP1) have been proposed.
Results: Various experimental approaches support a role for CCP1 in the removal of Glu residues from both α- and β-tubulin.
Conclusion: CCP1 functions in tubulin processing and is not involved in intracellular peptide degradation.
Significance: Neurodegeneration in mice lacking CCP1 is a result of altered tubulin processing.

The Purkinje cell degeneration (*pcd*) mouse has a disruption in the gene encoding cytosolic carboxypeptidase 1 (CCP1). This study tested two proposed functions of CCP1: degradation of intracellular peptides and processing of tubulin. Overexpression (2–3-fold) or knockdown (80–90%) of CCP1 in human embryonic kidney 293T cells (HEK293T) did not affect the levels of most intracellular peptides but altered the levels of α-tubulin lacking two C-terminal amino acids (delta2-tubulin) ≥5-fold, suggesting that tubulin processing is the primary function of CCP1, not peptide degradation. Purified CCP1 produced delta2-tubulin from purified porcine brain α-tubulin or polymerized HEK293T microtubules. In addition, CCP1 removed Glu residues from the polyglutamyl side chains of porcine brain α- and β-tubulin and also generated a form of α-tubulin with two C-terminal Glu residues removed (delta3-tubulin). Consistent with this, *pcd* mouse brain showed hyperglutamylation of both α- and β-tubulin. The hyperglutamylation of α- and β-tubulin and subsequent death of Purkinje cells in *pcd* mice was counteracted by the knock-out of the gene encoding tubulin tyrosine ligase-like-1, indicating that this enzyme hyperglutamylates α- and β-tubulin. Taken together, these results demonstrate a role for CCP1 in the processing of Glu residues from β- as well as α-tubulin *in vitro* and *in vivo*.

The protein named Nna1 (for nuclear neuronal protein induced by axotomy) was discovered in 2000 in a search for mRNAs induced when neuronal axons were severed (1). However, the name Nna1 is not particularly accurate, as the protein is localized to the cell cytosol, not the nucleus, and is not specifically expressed in neurons (2). Therefore, the name cytosolic carboxypeptidase 1 (CCP1)[3] was proposed to reflect the nomenclature of other members of the metallocarboxypeptidase gene family (2, 3). CCP1 has low amino acid sequence homology to well studied metallocarboxypeptidases such as carboxypeptidase A1 (CPA1) and carboxypeptidase E, and it is in a distinct subfamily with five other cytosolic carboxypeptidases, named CCP2 through CCP6 (2, 3). In 2002, Fernandez-Gonzalez *et al.* (4) found that the Purkinje cell degeneration (*pcd*) mouse mutation mapped to the CCP1 gene (*Agtpbp1*). In these mice, Purkinje cells degenerate 3–5 weeks after birth, although several other cell types show slower neurodegeneration (5, 6). The expression of wild-type (WT) CCP1 cDNA in Purkinje cells restored the viability of these cells (7, 8). By contrast, expression of point mutants in which residues thought to be important for carboxypeptidase activity were mutated did not restore Purkinje cell viability, suggesting that CCP1 is a functional carboxypeptidase (7, 8).

The deficiency of CCP1 in *pcd* mice leads to a number of cellular defects, including abnormal accumulation of polysomes in cerebellar Purkinje cells (9), affected transcription, and DNA repair in mitral cells of the olfactory bulb and cerebellar Purkinje cells (10, 11), endoplasmic reticulum stress in Purkinje cells (12), formation of axonal spheroids (13), mitochondrial dysfunction (14), elevated autophagy (15), and abnormal dendritic development (16). However, none of these studies addressed the primary function of CCP1 or attempted to identify its substrates. Previously, two potential functions for

* This work was supported, in whole or in part, by National Institutes of Health Grants DA-004494 (to L. D. F.), 1P20 DA026149 (to R. H. A.), and 1R01 CA124898 (to S. B. Horwitz). This work was also supported by the Uehara Memorial Foundation and Japan Society for the Promotion of Science Grants 23570209 and 23117517 (to K. I.).

[S] This article contains supplemental Figs. S1–S5, Table S1, and Movies S1–S3.

[1] To whom correspondence may be addressed: Dept. of Cell Biology and Anatomy, Hamamatsu University School of Medicine, 1-20-1 Handayama, Hamamatsu 431-3192, Japan. Tel.: 81-53-435-2085; Fax: 81-53-435-2468; E-mail: kikegami@hama-med.ac.jp.

[2] To whom correspondence may be addressed: Dept. of Molecular Pharmacology, Albert Einstein College of Medicine, 1300 Morris Park Ave., Bronx, NY 10461. Tel.: 718-430-4225; Fax: 718-430-8922; E-mail: lloyd.fricker@einstein.yu.edu.

[3] The abbreviations used are: CCP1, cytosolic carboxypeptidase 1; deTyr, detyrosinylated; *pcd*, Purkinje cell degeneration; HEK293T, human embryonic kidney 293T cells; Nna1, nuclear neuronal protein induced by axotomy; CPA1, carboxypeptidase A1; TTL, tubulin tyrosine ligase; TTLL, tubulin tyrosine ligase-like; CPO, carboxypeptidase O; polyE, polyglutamyl.

CCP1 were proposed, the processing of tubulin and the degradation of intracellular peptides (2, 17).

Tubulin undergoes a number of post-translational modifications (18–20). Most forms of mammalian α-tubulin are initially produced with a C-terminal Tyr residue encoded in the gene; this form is named "Tyr-tubulin." The Tyr is enzymatically removed to produce deTyr-tubulin (18, 21). The deTyr-tubulin can be converted back to Tyr-tubulin through the addition of Tyr by the enzyme tubulin tyrosine ligase (TTL) (22). Alternatively, the deTyr-tubulin can be converted to delta2-tubulin by the removal of C-terminal Glu (18, 23). Another post-translational modification of α-tubulin as well as β-tubulin involves the addition and removal of polyglutamyl (polyE) side chains (18, 24). Tubulin glutamylation is performed by some members of the family of TTL-like proteins (25–27). CCP4–6 were recently shown capable of removing polyE side chains from tubulin (28, 29).

Another potential function for an intracellular peptidase such as CCP1 is the cleavage of peptides formed by the proteasome, which cleaves proteins into peptides of ~5–20 amino acids. Although it is generally thought that aminopeptidases are the primary peptide-degrading enzymes within the cytosol, it is possible that carboxypeptidases are also involved. Recently, levels of many cytosolic peptides were found to be increased in adult *pcd* mouse brains (15). This finding suggested that CCP1 plays a role in the degradation of proteasome-generated peptides. However, studies on mice are complicated by potential secondary effects due to the loss of Purkinje cells and subsequent behavioral changes.

The major goal of this study was to evaluate these two potential functions for CCP1, tubulin processing and peptide degradation. Using a combination of *in vitro* assays, cell culture techniques, and studies in mice, we have found that tubulin processing is the primary function of CCP1, not peptide degradation. To study if CCP1 can directly process tubulin and to determine which tubulin isotypes it cleaves, we purified CCP1 and investigated its enzymatic activity toward both α- and β-tubulin using Western blotting and mass spectrometry to characterize the reaction products. Our results demonstrate that purified CCP1 is capable of cleaving Glu residues from the C terminus of α-tubulin and from the polyE side chain of both α- and β-tubulin. Moreover, our data indicate that CCP1 can remove the C-terminal Glu from delta2-tubulin to produce a new form of α-tubulin, delta3. Consistent with a role for CCP1 in tubulin deglutamylation, the *pcd* mouse brain shows hyperglutamylation of both α- and β-tubulin. The hyperglutamylation of both tubulins and subsequent Purkinje cell death can be corrected by the knock-out of *ttll1*, indicating that TTLL1 can add Glu residues on β-tubulin as well as α-tubulin. Taken together, our data show a role for CCP1 in the processing of Glu residues from α- and β-tubulin *in vitro* and *in vivo*.

EXPERIMENTAL PROCEDURES

Animals—A line of *pcd* mouse (BALB/cByJ- Agtpbp1$^{pcd\text{-}3J}$/J) was purchased from The Jackson Laboratory and bred within the Animal Institute Barrier Facilities at Albert Einstein College of Medicine and Hamamatsu University School of Medicine. *Ttll1* knock-out (Δ*Ttll1*) mouse was described previously (30). *pcd* heterozygotes and Δ*Ttll1* heterozygotes were mated to obtain *pcd*/Δ*Ttll1* double heterozygotes. The *pcd*/Δ*Ttll1* double mutant was generated through the mating of the obtained double heterozygotes. Animal use experiments were approved by the Institutional Animal Care and Use Committee of Albert Einstein College of Medicine (protocol 20090305) and the Animal Care and Use Committee of Hamamatsu University School of Medicine (protocols 2009043 and 2010053).

Quantitative Real Time PCR—Total RNA was isolated from human embryonic kidney 293T (HEK293T) cells and mouse brain regions using RNeasy mini kit and RNeasy lipid tissue kit, respectively (Qiagen, Valencia, CA). cDNA was synthesized from 2 μg of total RNA and random hexamers using the superscript III first strand kit (Invitrogen). Primers for human and mouse CCP1, CCP2, CCP3, CCP4, CCP5, CCP6, and glyceraldehyde-3-phosphate dehydrogenase (GAPDH) were designed and purchased from Invitrogen (supplemental Table S1 and supplemental Fig. S5*D*).

Power SYBR Green PCR Master Mix (Applied Biosystems, Invitrogen) was used to label with SYBR Green fluorescent tag. PCRs were carried out on a 7900HT real time thermal cycler (Applied Biosystems). The thermal cycling conditions were as follows: uracil-DNA glycosylase decontamination step at 50 °C for 2 min, a denaturing step at 95 °C for 10 min, and 40 cycles of 10 s at 95 °C, 20 s at 60 °C, and 30 s at 72 °C, followed by a dissociation curve stage at 95, 60, and 95 °C, each for 15 s. All samples were run in triplicate. Quantitative values were obtained from the threshold cycle number (*Ct*). The *Ct* value represents the cycle at which the SDS 2.1 software (Applied Biosystems) begins to detect the increase in the signal associated with an exponential growth of PCR products. ΔΔ*Ct* method was used to calculate the fold change in expression. GAPDH values were used as an internal control.

Cell Culture and Cell Transfection—The following human cell lines were used in this study: HEK293T, COLO205, H358, A549, MCF7, and HuH7. All the cells were grown in Dulbecco's modified Eagle's medium (Invitrogen) containing 10% fetal bovine serum (Invitrogen) and 1% penicillin/streptomycin (Invitrogen) in a humidified incubator at 37 °C in 5% CO_2.

To knock down CCP1, three stealth siRNAs were purchased from Invitrogen. The sequences for CCP1-specific siRNAs are as follows: siRNA1 (aaaccauggacugaugaaauaguuc) E15, siRNA2 (aaaccuguaagcaacaccuggucgc) E18, and siRNA3 (aauaauuagacucuggcauugcugu) E21 (Invitrogen AGTPBP1-HSS118525). Stealth RNAi negative control duplexes (Invitrogen) were used as a control.

For the peptidomics and studies of tubulin modifications, a human CCP1-His_6 construct was created. The PCR product of the coding region of CCP1 C terminus with specific oligonucleotides (forward: 5′-ccactcatgtattcggttcagg and reverse: 5′-gcggatcctcagtgatggtgatggtgatggctagcaggtaggtatgttcttga) was subcloned into PCR-Script (Stratagene, Agilent, Santa Clara, CA) digested with PflMI and BamHI and re-subcloned into the pcDNA3-CCP1 expression vector to introduce a NheI site followed by a His_6 sequence in the C-terminal region before the stop codon. The sequence of the coding region of each plasmid was verified.

Transfection of CCP1-His_6 plasmid or siRNA into HEK293T cells was performed with either HEKFectin or transfectin transfection reagent (Bio-Rad) following the manufacturer's protocol. For studies of CCP1 overexpression, transfected cells were grown at 37 °C for 2 days. For studies of the effects of CCP1 knockdown, siRNA-treated cells were incubated for either 3 or 6 days.

Quantitative Peptidomics—HEK293T cells were plated in 150-mm plates in Dulbecco's modified Eagle's medium containing 10% FBS the day before transfection and incubated at 37 °C at 5% CO_2 and 95% humidity. On the day of transfection, cells were at 30–40% confluence. Plates were transfected with CCP1 siRNA (mix of three oligonucleotides 10–20 nM each, Invitrogen) or control siRNA. After incubation for 72 h at 37 °C, cells were collected, washed four times in 30 ml of PBS by centrifugation for 5 min at 800 × *g* at 4 °C, and peptides extracted and labeled as described (31, 32). Briefly, extracted peptides were labeled with five different 4-trimethylammoniumbutyryl isotopic labels (31, 33). Duplicate samples treated with CCP1 siRNA were labeled with the D3- and D9-4-trimethylammoniumbutyryl, and triplicate control samples were labeled with D0-, D6-, and D12-4-trimethylammoniumbutyryl tags. After labeling, samples were pooled and filtered through a 10-kDa cutoff Amicon Ultracel filter (Millipore, Billerica, MA), treated with hydroxylamine, desalted using a PepClean™ C18 spin column (Pierce), and then eluted with 160 μl of 70% acetonitrile containing 0.5% trifluoroacetic acid. The samples were frozen, dried in a vacuum centrifuge, and kept frozen until mass spectrometry analysis.

Liquid chromatography/mass spectrometry was performed on a Q-TOF-Ultima mass spectrometer (Micromass, Waters) or an API Q-Star Pulsar-i quadrupole time-of-flight mass spectrometer (Applied Biosystems/MDS Sciex, Foster City, CA) with a Symmetry C18 trapping column (Waters) in tandem with a separating BEH 130-C18 column (Waters) and eluted with a water/acetonitrile, 0.1% formic acid gradient at 600 nl/min. The spectra obtained from the analysis were screened manually for the identification of groups of peaks representing peptides labeled with the different isotope tags. Raw data were converted to peak-list using the Mascot search engine (Matrix Science Ltd., Boston), and the results were manually interpreted to eliminate false positives, using criteria described previously (31, 34). The quantification was performed by calculation of the ratio of peak intensity between the values of the control and treated samples.

Western Blotting—Treated and control HEK293T cells were either collected and sonicated in lysis buffer (50 mM Tris-HCl, pH 8.0; 120 mM NaCl, 0.5% Nonidet P-40) containing phosphatase and protease inhibitors (100 mM NaF, 0.2 mM sodium orthovanadate, 10 μg/ml pepstatin, 3 μg/ml E64, and protease inhibitor mixture complete mini (Roche Applied Science)) or lysed directly on a plate with hot (>95 °C) lysis buffer containing 1% SDS. Equal aliquots (12 μg of protein for CCP1 and Tyr-tubulin analysis, 80 μg of protein for deTyr- and delta2-tubulin) were fractionated on a denaturing polyacrylamide gel and transferred to nitrocellulose membranes. Antibodies against Tyr- and delta2-tubulin (Millipore, 1:1000), deTyr-tubulin (Abcam, Cambridge, MA, 1:1000), and CCP1 (Proteintech Group, Chicago, IL, 1:1500) were used to probe membranes, and then membranes probed with anti-Tyr-tubulin were stripped using Western blot Stripping buffer (Thermo Scientific) and incubated with anti-α-tubulin (Sigma, 1:1000). Bands were visualized using IRDye-800-conjugated anti-mouse or anti-rabbit antibodies (Rockland Immunochemicals Inc., Gilbertsville, PA, 1:3000), and the band intensity was measured using the Odyssey Infrared Imaging System (LI-COR, Lincoln, NE). In the experiments with baculovirus, membranes were probed with tetra-His antibody (Qiagen, 1:2000).

The mouse brains were homogenized with a Teflon homogenizer in hypotonic buffer (50 mM Tris-HCl, pH 7.5; 1% Triton X-100) containing a protease inhibitor mixture, complete mini (Roche Applied Science) for SDS-PAGE. For two-dimensional electrophoresis, tissues were homogenized in buffer (7 M urea, 2 M thiourea, 4% CHAPS, 40 mM DTT, 2% immobilized pH gradient buffer, pH range 3.5–5.0). To separate tubulin subunits, SDS with 95% purity (Sigma; catalog no. L5750) was used, instead of commonly used highly pure SDS. In two-dimensional electrophoresis, the first isoelectric focusing was performed with Immobiline DryStrip gels of pH 3–5.6, 13 cm in length, and Multiphor II (GE Healthcare). Proteins separated in SDS-PAGE or two-dimensional electrophoresis were transferred to polyvinylidene fluoride membranes (Millipore). Antibodies against glutamylated tubulin (mAb GT335, a gift from Carsten Janke, Université Montpellier, France; 1:5000) (35), polyglutamylated tubulin (anti-polyE; a gift from Dr. Martin Gorovsky, University of Rochester, NY; 1:1500), α-tubulin (Lab Vision, Thermo Scientific, 1:10,000), β-tubulin (Lab Vision, 1:1000), CCP1 (Proteintech Group, 1:2000), GAPDH (mAb 6C5, Millipore, 1:3000), TTLL1 (1:5000) (30), and TTLL7 (1:5000) (26) were used to probe membranes. Horseradish peroxidase-conjugated secondary antibodies (Jackson ImmunoResearch, West Grove, PA) were used at 1:10,000 as secondary antibodies. Signals were visualized with enhanced chemiluminescence reagent (GE Healthcare), and detected with a charge-coupled device camera, LAS-3000mini (Fujifilm, Tokyo, Japan).

CCP1 Expression and Purification—For expression in Sf9 cells, the full-length CCP1-His_6 construct was subcloned into NotI-BamHI sites of pVL1392 (Pharmingen). Baculovirus was produced with Baculoplatinum DNA (Orbigen, San Diego) (36). Sf9 cells infected with WT virus or CCP1 were lysed in 50 mM phosphate buffer, pH 7.0, containing EDTA-free protease inhibitor mixture complete mini (Roche Applied Science). After centrifugation at 20,000 rpm for 30 min, soluble fractions were collected, supplemented with 0.5% Nonidet P-40 and 0.5 M NaCl, and incubated with TALON metal affinity resin (Clontech) for 30 min at 4 °C. Unbound proteins were washed with 50 mM phosphate buffer, pH 7.0, containing 0.5% Nonidet P-40, 0.5 M NaCl, and EDTA-free protease inhibitor mixture complete mini. Resin with bound CCP1-His_6 protein was placed in a column and eluted stepwise with 50 mM phosphate buffer containing 0.1 M NaCl, EDTA-free protease inhibitor mixture complete mini, and imidazole concentrations of 10, 20, and 80 mM.

Slot Blotting—To check enzymatic activity of WT and CCP1 fractions obtained during enzyme purification, 25 μl of each imidazole eluate were incubated with 5 μg of purified porcine

brain tubulin (Cytoskeleton Inc., Denver, CO) in 80 mM PIPES, pH 7, at 37 °C for 1 h. For the characterization of CCP1 enzymatic activity, only 80 mM imidazole eluates were used. In a typical assay, 2 or 6 μl of CCP1 eluate were incubated with 1.25 μg of purified porcine brain tubulin in 80 mM PIPES, pH 7, at 37 °C for 1 h. Control samples contained 80 mM imidazole elution buffer instead of CCP1 eluate. In the experiments with NaCl, both CCP1 and control samples were supplemented with NaCl to 100, 200, or 500 mM concentrations. In the pH-dependence experiments, both CCP1 and control samples were incubated at pH 6–8. To check the effect of inhibitors/activators on CCP1 activity, CCP1 and control samples were preincubated with 1 mM *o*-phenanthroline, $CoCl_2$ (Sigma), $CaCl_2$, citrate (Fisher), or GTP (Invitrogen) on ice for 30 min before addition of tubulin. To check CCP1 activity toward stabilized porcine brain tubulin, purified brain tubulin was preincubated with 5 μM paclitaxel (Sigma) for 15 min at 37 °C before addition of CCP1 or 80 mM imidazole elution buffer.

After incubation with tubulin, samples were applied to wet nitrocellulose membrane (GE Healthcare) using slot blot apparatus (HYBRI-SLOT™ Manifold 1052MM, Invitrogen). PolyE-tubulin was detected using polyclonal antibody raised against polyglutamylated tubulin (described above). Band visualization and intensity measurements were performed as described under "Western Blotting." Relative activity of CCP1 was calculated from the loss of polyE-tubulin (and loss of deTyr-tubulin in case of pH dependence test).

Tubulin Mass Spectrometry—Aliquots (25 μl) of the 80 mM imidazole CCP1 eluate were incubated with 5 μg of purified porcine brain tubulin in 80 mM PIPES, pH 7, at 37 °C for 1 h. CCP1 and tubulin proteins were separated in a denaturing polyacrylamide gel and then visualized with GelCode blue stain reagent (Thermo Scientific). Bands corresponding to tubulin were cut from the gel, destained in 50% acetonitrile in water at 37 °C for 30 min, dried by vacuum centrifugation, and then digested with CNBr (150 mg/ml in 70% formic acid) for 3.5 h in the dark at room temperature. CNBr and formic acid were removed by vacuum centrifugation in a Speedvac through three cycles of drying and resuspension. The digest was fractioned by reverse phase capillary HPLC (Ultimate 3000, Dionex, CA) followed by mixing with matrix automatically with a robot (Probot, Dionex, CA). Mass spectrometry analysis was carried out using an Applied Biosystems ABI 4800 Proteomics TOF/TOF Analyzer (Foster City, CA) in both positive and negative ion mode.

Microtubule Assay—Microtubules from HEK293T cells were prepared as indicated (37) with slight modifications. Briefly, cells grown for 2 days were permeabilized on a plate with "OPTimum for microtubule preservation" buffer (OPT: 80 mM PIPES, 1 mM $MgCl_2$, 0.5% Triton X-100, 10% glycerol, 5 μM taxol, pH 6.8) at 37 °C for 10 min. To produce deTyr-tubulin, half of the plates with microtubules were incubated with 40 ng/ml CPA1 (Sigma) in OPT buffer at 37 °C for 15 min. After intensive washes with warm OPT buffer, polymerized microtubules were treated with purified CCP1 diluted in OPT buffer (1:10) at 37 °C for 1 h, and then processed for either Western blot or immunostaining.

For Western blotting, microtubules were collected from the plate in hot (>95 °C) 1% SDS buffer and then analyzed as described above. For immunocytochemistry, microtubules were fixed with 4% paraformaldehyde in PBS at room temperature for 15 min, washed with PBS, blocked in 5% BSA in PBS for 1 h, and then incubated with anti-deTyr-tubulin (1:300, Abcam) or anti-delta2-tubulin (1:500, Millipore). After washing with PBS containing 0.2% Tween 20, microtubules were incubated with secondary Cy3-conjugated antibodies (Jackson ImmunoResearch) for 1 h, washed, and mounted in ProLong Gold antifade reagent (Invitrogen).

Immunohistochemistry—After dissection, mouse brains were immediately frozen on a steel block cooled with liquid nitrogen. The fresh frozen samples were sliced in a cryostat, CM1950 (Leica Microsystems Inc., Buffalo Grove, IL), at 10-μm thickness. The tissue sections were fixed with cold methanol at −20 °C, blocked with 5% goat serum, and then incubated with anti-MAP1 antibody (HM-1; 1:300) at 4 °C overnight. Signals were visualized by labeling the primary antibodies with AlexaFluor488-conjugated secondary antibody (Invitrogen). Nuclei were counter-stained with 4′,6-diamidino-2-phenylindole (Dojindo Laboratories, Kumamoto, Japan). Photographs were taken with a fluorescence microscope equipped with a charge-coupled device camera, C4742–95-12ER (Hamamatsu Photonics, Hamamatsu, Japan).

Animal Behavior Test—Three animals (age 8–20 months) of each genotype (*pcd* or *pcd*/Δ*Ttll1*) were used for testing athletic performance. The animals were first made to grasp a cord with their body on the downside of the cord, and their behaviors were then observed for 1 min. When animals climbed onto the top of the cord, the time to accomplish the task was recorded, and the performance was considered as "succeeded." When animals dropped from the cord or failed to climb onto the cord within the allotted time of 1 min, the athletic performance was considered as "failed."

RESULTS

CCP1 mRNA Is the Most Abundant CCP mRNA in HEK293T Cells—To study CCP1 function in a simple system, we searched for a cell line that expresses high levels of CCP1 mRNA and low levels of other CCP transcripts. We reasoned that a cell line with high levels of CCP1 mRNA and low levels of other CCP mRNAs would be suitable to study the consequences of CCP1 knockdown. Moreover, if cells express CCP1, then these cells should contain any co-factors and/or binding partners that may be necessary for CCP1 function. Thus, it would be useful to study the effect of CCP1 overexpression in this cell line. We performed quantitative real time-PCR on several human cell lines: HEK293T, COLO205, H358, A549, MCF7, and HuH7. Of these cell lines, the highest relative level of CCP1 mRNA was observed in HEK293T (Fig. 1*A*). The relative levels of all other CCP mRNAs in HEK293T cells were much lower than the level of CCP1 mRNA (Fig. 1*B*) and were either not detectable (CCP3, CCP4, and CCP6; data not shown) or present at low levels (CCP2 and -5; Fig. 1*B*). The knockdown of CCP1 mRNA with siRNA worked very well; treatment of cells with CCP1 siRNA for 3 or 6 days led to a significant decrease in CCP1 mRNA levels and did not cause any changes in the levels of CCP2 and

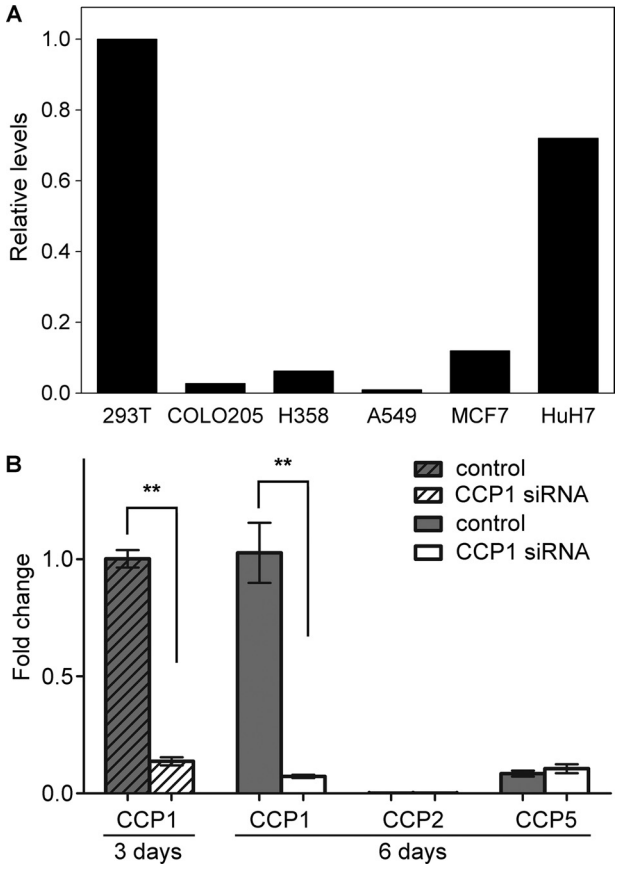

FIGURE 1. **High abundance of CCP1 mRNA in HEK293T cells and the specificity of CCP1 knockdown.** *A,* quantitative real time PCR was performed to determine CCP1 mRNA levels in HEK293T, COLO205, H358, A549, MCF7, and HuH7 human cell lines. The highest relative levels of CCP1 mRNA were observed in HEK293T cells. *B,* quantitative real time PCR was performed to determine mRNA levels of CCP1–6 in HEK293T cells after treatment with control dsRNA or CCP1 siRNA for 3 or 6 days, as indicated. For the 3-day treatment, only data for CCP1 are shown. For both time points, CCP3, CCP4, and CCP6 mRNAs were not detectable (data not shown). Treatment of cells with CCP1 siRNA for either 3 or 6 days leads to a significant decrease of CCP1 mRNA but does not affect mRNA levels of other CCPs. Fold change in expression was calculated using the $\Delta\Delta Ct$ method. GAPDH was used as an internal control. $n = 4$. *Error bars* represent means ± S.E. **, $p < 0.01$ using Student's *t* test.

CCP5 mRNAs (Fig. 1*B*) or the levels of CCP3, CCP4, and CCP6 transcripts (data not shown). Thus, the other CCPs are not up-regulated to compensate for the decrease in CCP1. Altogether, these data suggest that the HEK293T cell line is an appropriate system to study the role of CCP1.

Levels of Most Peptides Are Not Affected after CCP1 Knockdown or Overexpression in HEK293T Cells—Previously, a large number of peptides derived from cytosolic and mitochondrial proteins were found to be greatly elevated in amygdala, hypothalamus, cortex, and striatum of *pcd* mutant mice, relative to WT mice (15). A graphic summary of the relative levels of hypothalamic peptides in *pcd* and WT mice is shown in Fig. 2*A*. One interpretation of the increased levels of many peptides in *pcd* mouse brain regions was that CCP1 functions in the degradation of peptides produced by the proteasome (15). Alternatively, the changes in cellular peptide levels could be a secondary response and not reflect the primary function of CCP1. To test these two hypotheses, we performed quantitative peptidomics of HEK293T cells after treatment with CCP1 siRNA, compared with untreated control cells. The relative levels of all detected peptides in the control cells are shown in Fig. 2*B* (*black line*). CCP1 knockdown caused a slight increase in the level of some peptides (Fig. 2*B*, *upper gray line*), but the effect was much less dramatic than the large increase in many peptides seen in the *pcd* mouse brain regions (Fig. 2*A*). Conversely, CCP1 overexpression caused a slight decrease in the levels of some peptides (Fig. 2*B*, *lower gray line*). Further analysis showed that of the hundreds of peptides detected in the analysis, only seven showed a statistically significant increase in the CCP1 siRNA samples, and no peptides showed a statistically significant decrease in the CCP1 overexpression samples (Fig. 2*C*). The fact that only a handful of peptides showed an apparent increase with CCP1 knockdown and none of these showed the opposite change after CCP1 overexpression suggests that degradation of intracellular peptides is not the primary role of CCP1.

CCP1 Removes Glutamates from Tubulin C Termini in HEK293T Cells—Tubulin is a dynamic molecule that undergoes different post-translational modifications that are important for regulation of the microtubule cytoskeleton. To investigate the role of CCP1 in the dynamics of endogenous HEK293T tubulin, we transfected cells with plasmids expressing CCP1 and analyzed the levels of CCP1 protein and the different tubulin modifications. CCP1 protein levels were increased ~5-fold after transfection (Fig. 3*A*, *top row*). The levels of Tyr- and deTyr-tubulin were not changed in HEK293T cells after CCP1 mRNA overexpression. Levels of delta2-tubulin were significantly elevated after CCP1 overexpression (Fig. 3, *A* and *B*). PolyE-tubulin was not examined because these forms of tubulin are undetectable in HEK293T cells (supplemental Fig. S1).

To check if CCP1 knockdown causes the opposite effect on tubulin forms, we treated HEK293T cells with either control or CCP1 siRNA and studied modifications of endogenous cell tubulin. CCP1 protein levels are substantially decreased by the siRNA treatment (Fig. 3*C*, *top row*). As with CCP1 overexpression, we did not observe any changes in Tyr- and deTyr-tubulin levels upon siRNA treatment (Fig. 3, *C* and *D*). However, levels of delta2-tubulin were significantly decreased by the CCP1 knockdown. Collectively, our data suggest that CCP1 cleaves the Glu residue from deTyr-tubulin to form a pool of delta2-tubulin. These results are consistent with a recent study that was published while our studies were ongoing (29).

Characterization of CCP1 Activity toward Purified Porcine Brain Tubulin—Because the levels of endogenous polyE-tubulin are undetectable in HEK293T cells, these cells are not a suitable system to study the activity of CCP1 toward this form of tubulin. Thus, we used purified porcine brain tubulin to study the enzymatic activity of CCP1 toward polyE modifications. Using the baculovirus expression system, we expressed CCP1-His_6 in Sf9 insect cells and then purified the enzyme using a metal affinity column, which exhibits high affinity for His-tagged proteins. We obtained a fraction highly enriched in CCP1 (supplemental Fig. S2). The imidazole eluates were incubated with brain tubulin for 2 h, and levels of polyE-tubulin were analyzed using an antibody that recognizes polyE side chains. We observed a decrease in polyE-tubulin only in samples treated with the 80 mM imidazole eluates (Fig. 4, *A* and *B*),

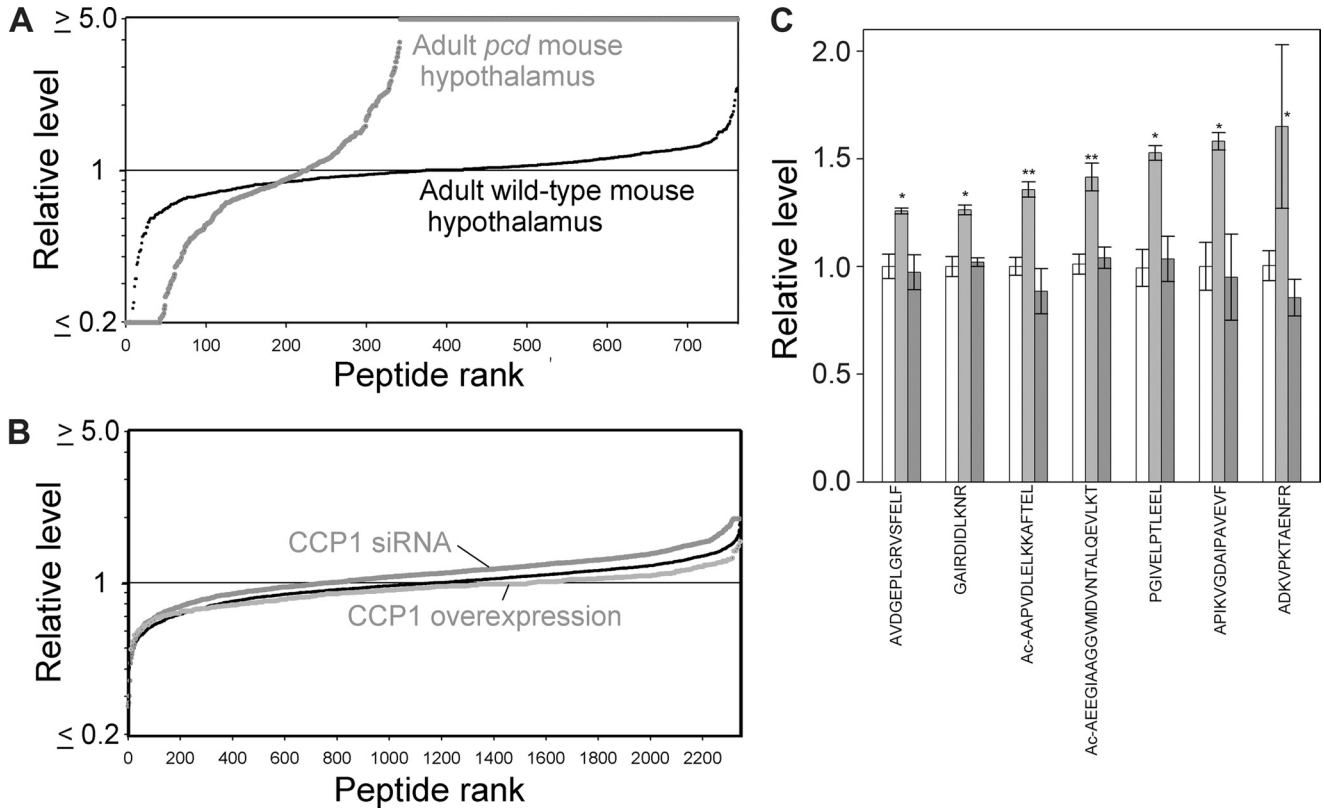

FIGURE 2. **Effect of CCP1 on peptide levels in HEK293T cells and WT and *pcd* mice.** Quantitative peptidomics was used to analyze the levels of peptides derived from cytosolic and mitochondrial proteins. *A,* relative levels of peptides in the hypothalamus of adult WT and *pcd* mice. Each *dot* in the graph represents the ratio of a peptide in one replicate of the indicated group *versus* the average level in the WT replicates. *Small black circles* show the WT/WT ratio; *larger gray circles* represent the *pcd*/WT ratio. The *y* axis is logarithmic and is capped at either 5-fold decreases (ratio ≤0.2) or increases (ratio ≥5). The *x* axis represents the relative rank order of each peptide, compared with all other peptides detected in the study. *B,* relative levels of peptides in control HEK293T cells, in cells overexpressing CCP1, and in siRNA-treated HEK293T cells. Each *dot* in the graph represents the relative level of an individual peptide in one replicate of the indicated group *versus* the average level of that peptide in the control groups for that experiment. The *thin black line* (*i.e.* the *small black circles*) shows the control/control ratio, the *lower light gray line* shows the ratio for CCP1 overexpression/control; and the upper *dark gray line* shows the ratio for CCP1 siRNA/control. *C,* effect of CCP1 knockdown or overexpression on the level of individual peptides. Levels of peptides detected by peptidomics of HEK293T cells after CCP1 knockdown and overexpression were analyzed and compared with controls pooled from both experiments. *Graph* shows the relative levels of those peptides that showed statistically significant changes after CCP1 knockdown for 3 days compared with controls. VVRHQLLKT is derived from cytochrome *c* oxidase subunit 7c; AVDEPLGRVSFELF, KHTGPGILSM, and ADKVPKTAENFRAL from peptidylprolyl isomerase A; GAIRDIDLKNR from splicing factor, arginine/serine-rich 1; MTEEAAVAIKAMAK from eukaryotic translation initiation factor 5A; Ac-AAPVDLELKKAFTEL from prefoldin subunit 1; Ac-AEEGIAAGGVMDVN-TALQEVLKT from of 40 S ribosomal protein S12; PGIVELPTLEEL from NADH dehydrogenase 1α subcomplex, 8; and APIKVGDAIPAVEVF from peroxiredoxin 5. $n = 6$ for controls, $n = 2$ for K_D/overexpression. *, $p \leq 0.05$; **, $p \leq 0.01$ *versus* pooled controls using two-tailed Student's *t* test.

which corresponds to the fraction enriched with CCP1 protein (supplemental Fig. S2). These data suggest that CCP1 is an active enzyme that is capable of cleaving side chain Glu residues from polyE-tubulin.

The enzymatically active CCP1 in the 80 mM imidazole eluates of the metal affinity column was further characterized. To determine the optimal pH range for CCP1, we incubated the enzyme with brain tubulin at pH 6–8. CCP1 activity was calculated from the loss of Glu from either polyE or deTyr tubulin. CCP1 exhibited maximal activity toward polyE and deTyr-tubulin at pH 6–7 (Fig. 4*C*). CCP1 activity was maximal in the absence of NaCl (Fig. 4*D*).

CCP1 is in the metallocarboxypeptidase family and therefore is expected to require metal ions for enzyme activity. To test this, we incubated CCP1 with brain tubulin in the presence or absence of *o*-phenanthroline, a chelator of divalent cations. Levels of polyE and α-tubulin were analyzed by Western blot. *o*-Phenanthroline substantially inhibited CCP1 activity toward polyE-tubulin (Fig. 4, *E* and *F*), which is consistent with the expected properties of a metallopeptidase. Furthermore, CCP1 activity was enhanced by $CoCl_2$ (Fig. 4*G*), an activator of other metallocarboxypeptidases (38, 39). Interestingly, $CaCl_2$ produced a slight activation (Fig. 4*G*); this ion has a small effect on some metallocarboxypeptidases (40). CCP1 activity was not affected by citric acid (Fig. 4*G*), which has some chemical similarities to glutamate, weakly inhibits carboxypeptidase A1 (41), and potently inhibits CPO (42). GTP was also tested because it was proposed that CCP1 has an ATP/GTP-binding motif (1), and it was previously reported that GTP activates the related enzyme CCP6 (3). However, CCP1 does not show any activation by GTP (Fig. 4*G*).

CCP1 Cleaves Glu from Side Chains of Both α- and β-Tubulin and Can Also Form delta3-Tubulin—A recent paper from Rogowski *et al.* (29) and our experiments with the anti-polyE antibody (Fig. 4) suggest that CCP1 cleaves Glu residues from polyE-tubulin. To confirm this, we incubated purified CCP1 with porcine brain tubulin and performed mass spectrometry following cyanogen bromide fragmentation. We were able to detect C-terminal peptides of both α- and β-tubulin. The peptides were derived from the tubulin isotypes β2b, β2c, α4a, α1c,

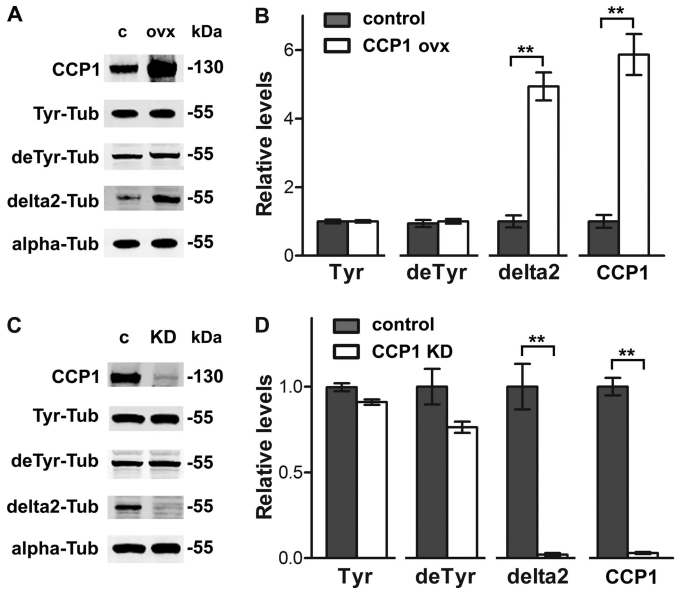

FIGURE 3. **α-Tubulin processing in HEK293T cells after CCP1 overexpression or knockdown.** *A,* representative Western blots for CCP1 protein and different forms of α-tubulin in HEK293T cells after overexpression of His_6-tagged CCP1. *B,* densitometric analysis of the levels of CCP1 protein and different tubulin forms in control and CCP1-overexpressing HEK293T cells. The Tyr-, deTyr-, and delta2-tubulin band densities were normalized with the corresponding α-tubulin bands. Band densities were measured using the Odyssey infrared imaging system. The levels of delta2-tubulin are significantly increased in HEK293T cells after CCP1 overexpression for 2 days, whereas other tubulin modifications are not affected. *Error bars* represent mean ± S.E. ($n = 4$). **, $p < 0.01$ using Student's *t* test. *C,* representative Western blots for CCP1 protein and different forms of α-tubulin after treatment of cells with CCP1 siRNA for 3 days. *D,* densitometric analysis of the levels of CCP1 protein and different tubulin forms in control and siRNA-treated HEK293T cells. The Tyr-, deTyr-, and delta2-tubulin band densities were normalized with the corresponding α-tubulin bands. The levels of delta2-tubulin are significantly decreased in HEK293T cells after CCP1 mRNA knock down for 3 days. *Error bars* represent mean ± S.E. ($n = 4$). **, $p < 0.01$ using Student's *t* test. Abbreviations used are as follows: *c*, control; *KD*, knockdown; *ovx,* overexpression; *Tub*, tubulin.

and α1a/α1b/α3 (these three peptides have the same sequence and mass and cannot be distinguished).

The ion peak with *m/z* 2567.08 (Fig. 5*A*) corresponds to the C-terminal peptide of delta2 α1a/α1b/α3-tubulin. Additional peaks with masses +129 Da are observed, indicating that delta2 α-tubulin is polyglutamylated. MS/MS data confirmed the identity of the 2696 and 2825 ions as C-terminal fragments of α1a/α1b/α3-tubulin (supplemental Fig. S3*A*). Incubation of brain tubulin with CCP1 shifted the balance to tubulin forms with fewer Glu residues on the side chain (Fig. 5*A*, *middle panel*). Interestingly, we detected a new form of α-tubulin lacking all Glu residues from both the C terminus and side chain of α1a/α1b/α3 (2438.05 Da, Fig. 5*A*, *middle panel*) and α4a (data not shown). These results suggest that CCP1 removes the C-terminal Glu from delta2 to form delta3-tubulin. As a positive control for Glu cleavage, we incubated tubulin with purified carboxypeptidase O (CPO) (Fig. 5*A*, *bottom panel*). CPO is a member of the A/B subfamily of metallocarboxypeptidases that removes C-terminal acidic residues from peptides and proteins, and it is not known to cleave γ-linked branch point Glu residues (42). When incubated with porcine brain tubulin and analyzed by mass spectrometry, CPO was also capable of producing delta2 and delta3 (Fig. 5*A*, *bottom panel*). However, the levels of delta3 after CPO treatment were much lower than after incubation with CCP1, consistent with the interpretation that CPO removes only α-linked Glu residues and not the branch point Glu, whereas CCP1 removes both C-terminal Glu residues and the branch point Glu from α-tubulin. Similar changes were observed with the α4a tubulin isotype after incubation with CCP1 (data not shown). Taken together, these data confirm that CCP1 removes Glu from polyE α-tubulin.

The major forms of β2b-tubulin were with side chain of 1–2 Glu residues (Fig. 5*B*, *upper panel*, masses of 3594.42 and 3723.43 Da, respectively, and supplemental Fig. S3*B*). After treatment of tubulin with CCP1, the peak corresponding to the deglutamylated form of β2b was increased compared with control (Fig. 5*B*, *middle panel*, mass 3465.34 Da), suggesting that CCP1 cleaves the side chain Glu to form the deglutamylated form of β2b-tubulin. CPO is not able to remove branch point Glu from the side chain of β-tubulin 2b (Fig. 5*B*, *bottom panel*). The β2c isoform also showed the same shift toward the deglutamylated form after treatment with CCP1 (supplemental Fig. S4). Collectively, our data indicate that CCP1 cleaves the side chain Glu from both α- and β-tubulin.

CCP1 Can Function on Polymerized Tubulin—Post-translational modifications such as detyrosination and the generation of delta2-tubulin are linked to microtubule stability (43). To test whether CCP1 is active toward polymerized tubulin, we prepared microtubules from HEK293T cells, treated some of the samples with CPA1 to increase the level of deTyr tubulin, and then incubated with purified CCP1. Tubulin forms were analyzed either by Western blot (Fig. 6, *A* and *B*) or by immunofluorescence (Fig. 6*C*). When CCP1 was incubated with polymerized microtubules, the enzyme produced delta2 (Fig. 6, *A–C*). A similar effect was seen in the absence of CPA1 treatment (Fig. 6, *A* and *B*). These results indicate that CCP1 can function on polymerized tubulin.

To study if tubulin polymerization affects CCP1 activity, we treated purified porcine brain tubulin with CCP1 in the presence or absence of taxol, a drug that stabilizes microtubules (44). CCP1 was able to cleave Glu from polyE side chains and the C terminus of tubulin in the presence and absence of taxol (Fig. 6*D*). The levels of delta2-tubulin decreased after CCP1 treatment, which is consistent with our data obtained by mass spectrometry. This suggests that CCP1 produces the delta3 form by removing C-terminal Glu from delta2-tubulin. Interestingly, the activity of CCP1 toward polyE-tubulin was not affected by taxol, whereas the activity toward delta2-tubulin was slightly reduced in the presence of taxol (Fig. 6*D*).

Loss of CCP1 Results in Hyperglutamylation of β-Tubulin as Well as α-Tubulin in Vivo—Given that both α- and β-tubulin polyE side chains were processed by CCP1 *in vitro*, we hypothesized that the loss of CCP1 in *pcd* mice would cause the hyperglutamylation of α- and β-tubulin *in vivo*. To test this, extracted proteins from adult *pcd* and WT mouse olfactory bulb, cerebrum, and cerebellum were subjected to SDS-PAGE to separate α- and β-tubulin, and Western blot analyses were performed. The monoclonal antibody GT335 showed a slightly decreased signal for α-tubulin in the *pcd* mouse brain samples, relative to the WT mice (Fig. 7, *A* and *B*). This antibody recognizes the branch point of glutamylated tubulin and shows optimal bind-

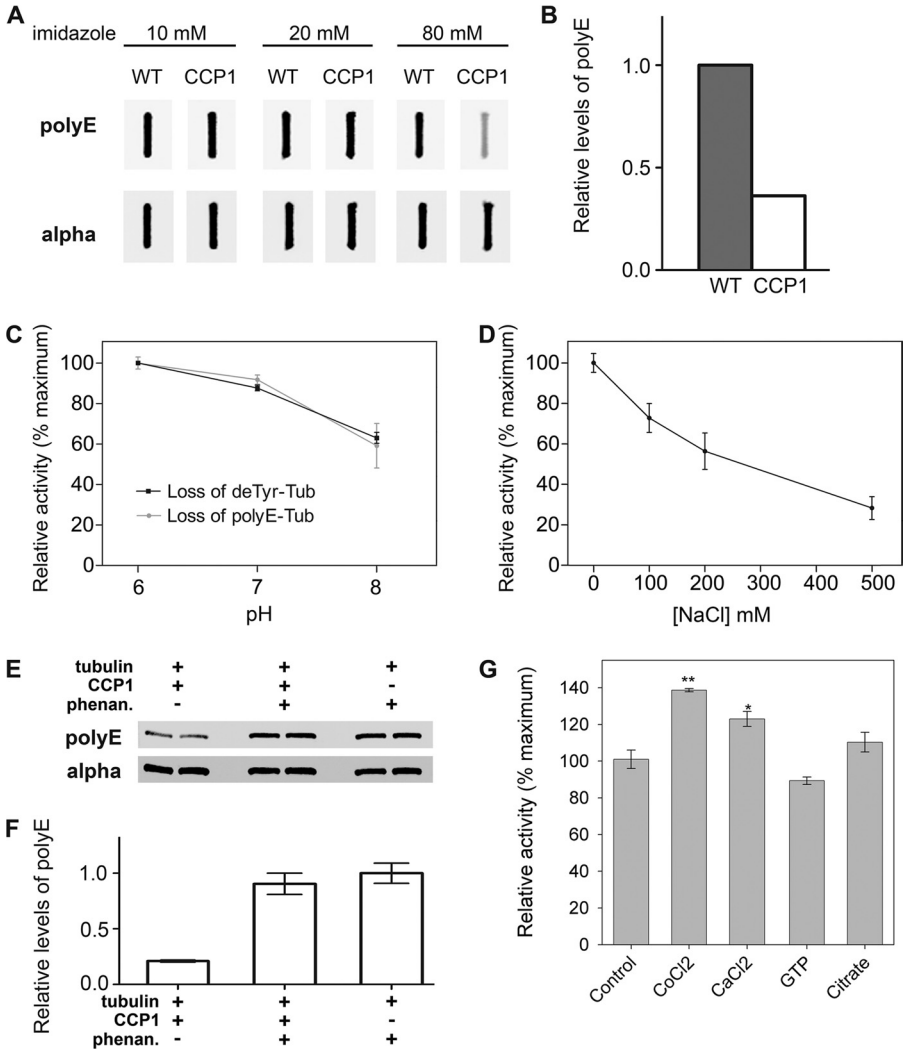

FIGURE 4. **Characterization of CCP1 enzymatic activity toward purified brain tubulin.** *A,* Sf9 cells infected with either wild-type (*WT*) baculovirus or CCP1-expressing baculovirus were eluted from a metal affinity column with buffers containing 10, 20, or 80 mM imidazole. The eluates were incubated with purified porcine brain tubulin at 37 °C for 2 h. After incubation, samples were slot-blotted into the nitrocellulose membrane and probed with either polyE or α-tubulin antibody. *B,* densitometric analysis of polyE-tubulin levels after treatment with 80 mM eluates from either the WT virus or CCP1-expressing virus. The polyE-tubulin band densities were normalized with the corresponding α-tubulin bands. Although the initial screening of the column fractions was performed a single time, the 80 mM imidazole eluate from the CCP1-expressing virus was used for the subsequent studies in this figure, each of which was performed in replicates. *C,* effect of pH on CCP1 activity toward porcine brain tubulin. Purified CCP1 was incubated with purified tubulin (*Tub*) at different pH values for 1 h, and then samples were slot-blotted into nitrocellulose membrane and probed with deTyr- ($n = 3$) and polyE-tubulin antibodies ($n = 6$). *Error bars* represent means ± S.E.. *D,* effect of NaCl on CCP1 activity toward porcine brain tubulin. Purified CCP1 was incubated with purified tubulin at pH 7 for 1 h at different concentrations of NaCl. Samples were slot-blotted onto nitrocellulose membrane, and CCP1 activity was measured as loss of polyE-tubulin. *Error bars* represent means ± S.E. ($n = 3$). *E* and *F,* purified CCP1 was incubated with purified brain tubulin at pH 7 for 1 h in the presence or absence of 10 mM *o*-phenanthroline (*phenan*). *E,* representative Western blots for polyE and α-tubulin. *F,* densitometric analysis of levels of polyE-tubulin ($n = 2$). The band densities were normalized with the corresponding α-tubulin bands. *G,* purified CCP1 was incubated with purified tubulin at pH 7 for 1 h in the presence of 1 mM $CoCl_2$, $CaCl_2$, GTP, or citrate. Samples were blotted into nitrocellulose membrane and CCP1 activity was measured as loss of polyE-tubulin. *Error bars* represent means ± S.E. ($n = 3$). *, $p < 0.05$; **, $p < 0.01$ *versus* control, using Student's *t* test.

ing to forms of tubulin with short polyE side chains (35). In contrast, the polyclonal antiserum anti-polyE showed a stronger signal for α- and β-tubulin in the *pcd* mouse brain samples, especially in the olfactory bulb and cerebellum, compared with WT samples (Fig. 7, *A* and *B*). This antiserum recognizes longer chains of polyE (45, 46). These results indicate that the loss of CCP1 results in hyperglutamylation of β-tubulin as well as α-tubulin. As reported by Rogowski *et al.* (29), the level of delta2-tubulin was not significantly changed in the adult *pcd* brain (Fig. 7, *A* and *B*).

To examine more clearly whether α- and β-tubulins are hyperglutamylated in *pcd* brain, we carried out two-dimensional electrophoresis, followed by Western blot analysis with mAb GT335. In the two-dimensional electrophoresis, we analyzed proteins extracted from olfactory bulb, because the sample of olfactory bulb showed the most marked change in one-dimensional Western blot analysis. Consistent with the result shown in Fig. 7, *A* and *B*, β-tubulin of *pcd* olfactory bulb migrated to the more acidic side, relative to WT samples (Fig. 7*C, arrow*), indicating the hyperglutamylation of β-tubulin in *pcd* mouse olfactory bulb. The forms of α-tubulin in *pcd* tissue also shifted toward the acidic side, relative to WT tissue (Fig. 7*C*).

We also examined whether TTLL1 and TTLL7 were increased in the *pcd* brain. We selected these two TTL-like

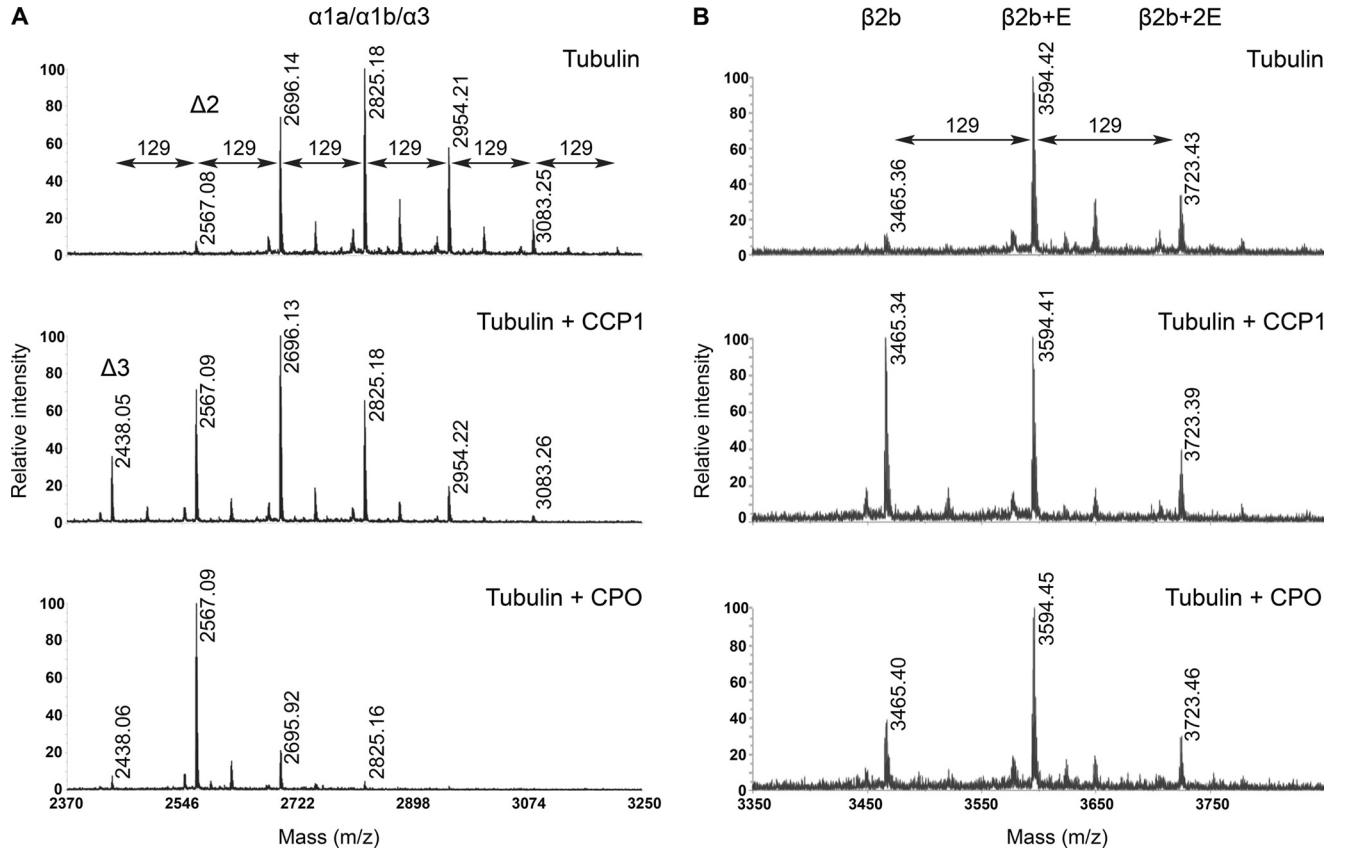

FIGURE 5. **Tubulin processing by purified CCP1.** *A,* representative spectra of α1a/α1b/α3 forms of porcine α-tubulin. After incubation, tubulin was isolated on polyacrylamide gel, digested with CNBr, and analyzed as described. The form shown is the C-terminal region of α1a/α1b/α3. *Top panel,* spectrum of α1a/α1b/α3 brain tubulin alone. *Middle panel,* spectrum of α1a/α1b/α3 brain tubulin after incubation with purified CCP1. *Bottom panel,* spectrum of α1a/α1b/α3 brain tubulin after incubation with CPO. *B,* representative spectra of β2b form of porcine β-tubulin. After incubation, tubulin was isolated on a polyacrylamide gel, digested with CNBr, and analyzed as described. The form shown is the C-terminal region of β2b. *Top panel,* spectrum of β2b brain tubulin alone. *Middle panel,* spectrum of β2b brain tubulin after incubation with purified CCP1. *Bottom panel,* spectrum of β2b brain tubulin after incubation with CPO. The molecular mass of a Glu residue is 129 Da.

proteins because TTLL1 is the catalytic subunit of the main enzyme for α-tubulin glutamylation in brain (25, 47), and TTLL7 is a main enzyme for β-tubulin glutamylation in neuronal tissues (26). Levels of TTLL1 and TTLL7 were comparable between WT and *pcd* mice when olfactory bulb and cerebrum were examined (Fig. 7, *D* and *E*). In *pcd* cerebellum, TTLL1 and TTLL7 tended to be slightly decreased, relative to WT levels, although statistically significant differences were not detected (Fig. 7, *D* and *E*). These results indicate that the hyperglutamylation of α- and β-tubulin did not result from overproduction of TTLL1 or TTLL7.

In addition, we investigated the levels of CCP mRNAs in the amygdala, hypothalamus, and striatum of WT and *pcd* mice. Although in these brain regions CCP1 mRNA is a major transcript among CCPs in WT mice (2), neurons in these regions do not degenerate in CCP1 mutant *pcd* mice. To test the possibility that other CCPs compensate for the absence of CCP1 in *pcd* mice, we performed quantitative real time PCR on these brain regions of adult animals. CCP1 mRNA is the most abundant transcript among CCPs in the brain of WT mice (supplemental Fig. S5). The levels of CCP1 mRNA are lower in *pcd* compared with WT mice (supplemental Fig. S5), which is in agreement with previously reported results (4). Although CCP1 transcript is produced in *pcd* mice, CCP1 protein is not detectable (Fig. 7*A*). The levels of other CCP mRNAs are not affected by CCP1 mutation, indicating that there is no compensation by these other CCPs at the transcriptional level for the absence of CCP1 in *pcd* mice.

β-Tubulin Hyperglutamylation in pcd Brain Is Counteracted by Deletion of TTLL1—In neuronal tissues, polyglutamylation of α-tubulin is thought to be performed almost entirely by TTLL1 (25, 26, 47). Thus, we examined if TTLL1 is involved in the hyperglutamylation detected in the *pcd* brain. To this end, we generated double mutant mice for *pcd* and *Ttll1* knock-out (*pcd*/Δ*Ttll1*). The glutamylation of α-tubulin was decreased in the double knock-out mice to a level below that of WT samples (Fig. 8, *A* and *B*). This is consistent with previous reports that TTLL1 is selective for glutamylation of α-tubulin (25, 47). Unexpectedly, the hyperglutamylation of β-tubulin detected in the *pcd* brain was reduced and almost reached the same level as WT by the deletion of TTLL1 (Fig. 8, *A* and *B*). These results suggest that TTLL1 is involved in hyperglutamylation of both β- and α-tubulin and that the deletion of TTLL1 is sufficient for counteracting the hyperglutamylation in *pcd* mouse brain.

Given that *Ttll1* knock-out reversed hyperglutamylation by the CCP1 loss, we next examined if *Ttll1* knock-out could rescue the degeneration of Purkinje cells in *pcd* mice. We prepared fresh-frozen sections of 10 μm in thickness from 8-week-old

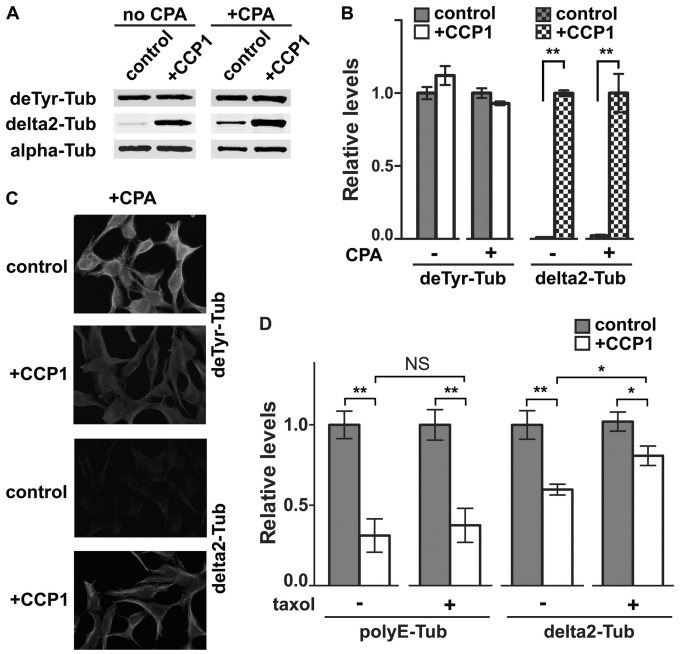

FIGURE 6. **CCP1 activity toward polymerized tubulin.** HEK293T cells were treated on plates with microtubule-stabilizing buffer containing 5 μM taxol, and then half of the plates were treated with CPA1 (40 ng/ml) to convert Tyr-tubulin into deTyr-tubulin. After intensive washes to remove the CPA1, polymerized microtubules were treated with purified CCP1 for 1 h and then processed for either Western blot or immunostaining. *A,* representative Western blots for different forms of α-tubulin after treatment of microtubules with purified CCP1. *B,* densitometric analysis of different tubulin forms after treatment of polymerized microtubules with purified CCP1. The deTyr- and delta2-tubulin band densities were normalized with the corresponding α-tubulin bands. The levels of delta2-tubulin are significantly increased after CCP1 treatment, whereas other forms of tubulin are not affected. *Error bars* represent means ± S.E. ($n = 4$). **, $p < 0.01$ *versus* control using Student's *t* test. *C,* immunofluorescence analysis of polymerized microtubules after treatment with CPA1 and then with CCP1. Polymerized control or CCP1-treated microtubules were subjected to immunostaining with antisera against deTyr- and delta2-tubulin. *D,* purified brain tubulin was incubated with CCP1 in the presence or absence of 5 μM taxol. Samples were processed for Western blot, and densitometric analysis of polyE and delta2-tubulin forms was performed. The levels of polyE and delta2-tubulin significantly decreased after CCP1 treatment in either the absence (−) or presence (+) of taxol. *, $p < 0.05$; **, $p < 0.01$ using Student's *t* test. *NS*, not significant. *Tub*, tubulin.

pcd and *pcd*/Δ*Ttll1* mouse cerebellum and then stained them with anti-MAP1 antibody to detect Purkinje cells. This immunochemical staining showed the survival of Purkinje cells in the *pcd*/Δ*Ttll1* double mutant mouse (Fig. 8*C*). Whereas no Purkinje cells were observed in the 8-week *pcd* cerebellum (Fig. 8*C, left panel*), there remained many Purkinje cells in the 8-week *pcd*/Δ*Ttll1* double mutant cerebellum (Fig. 8*C, right panel*).

As we observed that Purkinje cells still remained in the 8-week *pcd*/Δ*Ttll1* cerebellum, we examined whether the ataxic behavior observed in *pcd* mice was improved in the *pcd*/Δ*Ttll1* double mutant. Animals were allowed to grasp a cord with their bodies on the downside of the cord (supplemental Movie S1), and then their behaviors were recorded for 1 min (supplemental Movie S1). The time it took for the animals to successfully climb onto the cord was measured (Fig. 8*D*). When animals failed to climb onto the cord within 1 min, or dropped from the cord, the athletic performance was considered as "failed." We analyzed three independent mice for each of *pcd* and *pcd*/Δ*Ttll1* animals, including one 5-month-old mouse. All the *pcd*/Δ*Ttll1* mice succeeded in climbing on the cord within 20 s (supplemental Movie S1), whereas none of the *pcd* mice accomplished this task; two *pcd* mice failed to climb within the allotted time of 60 s (supplemental Movies S2 and S3), and one *pcd* animal dropped from the cord (Fig. 8*D*). These results clearly demonstrate that the *pcd* mouse, even at 20 weeks, is rescued from ataxia by TTLL1 deletion.

DISCUSSION

It has been ~40 years since the discovery of the *pcd* mouse (5) and ~10 years since the finding that these mice contain a mutation in the *Agtpbp1* gene, which produces CCP1 protein (4). During this time, a large number of mechanisms have been proposed to explain the Purkinje cell death, including altered DNA repair, mitochondrial function, autophagy, organelle shape, and others. Several of the authors of this study previously speculated that CCP1 was involved in peptide turnover because large increases in cytosolic peptide levels were found in many regions of the *pcd* mouse brain (15). The possibility that CCP1 functions in tubulin processing was also proposed (2). However, it is important to distinguish the primary action of CCP1 from secondary effects that result from the primary deficiency. The goal of this study was to investigate the functions of CCP1 in three different systems: a cell culture system using short term overexpression and knockdown of the protein; *in vitro* analysis of purified enzymes and substrates; and *in vivo* studies using *pcd* mice.

One of the systems we chose, HEK293T cells, expresses relatively high levels of CCP1 compared with other cell lines examined but only low levels of the other members of the CCP subfamily, thereby reducing the possibility that the other CCPs could compensate for the alterations in CCP1 levels. Using this system and a quantitative peptidomics technique, we found that overexpression and knockdown of CCP1 did not affect the levels of most intracellular peptides. This finding suggests that the previous peptidomics results from *pcd* mouse brain reflect a secondary change and that CCP1 is not primarily involved in peptide degradation.

In contrast to the peptide data, the analysis of tubulin forms showed consistent results implicating CCP1 in the removal of Glu from the C terminus of α-tubulin. The opposing results with overexpression and knockdown of CCP1 on levels of delta2-tubulin add credence to the results. Although it was anticipated that levels of deTyr tubulin would also be affected by CCP1 overexpression or knockdown, this form is in dynamic equilibrium with the Tyr form due to a tubulin tyrosine ligase present in HEK293T cells. Furthermore, the levels of the Tyr and deTyr forms are much higher than the levels of the delta2 form in HEK293T cells, and so large changes in the levels of the delta2 forms are not necessarily reflected by comparable changes in the levels in the more abundant forms. The *in vitro* studies with partially purified CCP1 and purified brain tubulin clearly show that CCP1 cleaves C-terminal Glu from α-tubulin and from the polyE side chains of both α- and β-tubulin. While our study was in progress, another group reported that CCP1 overexpression in HEK293T cells affected levels of delta2-tubulin (29). Our studies with HEK293T cells are consistent with these recently published studies, and our work with purified

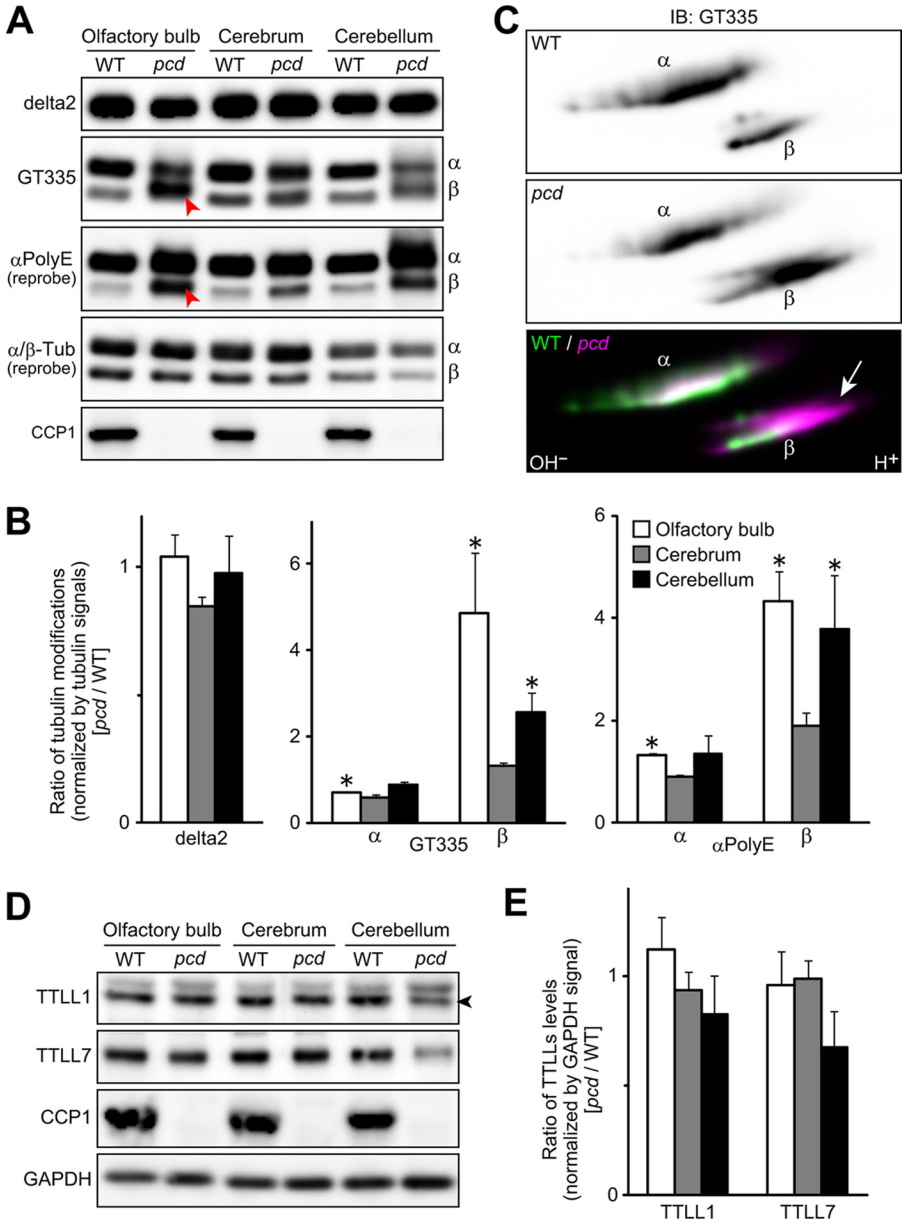

FIGURE 7. **Hyperglutamylation of β-tubulin as well as α-tubulin in adult *pcd* brain.** *A,* representative Western blots for glutamylated α- and β-tubulins and CCP1. Glutamylated or polyglutamylated tubulin (*Tub*) was detected with GT335 or αpolyE, respectively. *Arrowheads* highlight increases of β-tubulin band intensities detected by GT335 and αpolyE in olfactory bulb. α- and β-tubulins were detected with independent antibodies, and so the relative intensities of the two forms do not appear identical. *B,* quantitative analysis of tubulin modifications in the *pcd* brain. Results are shown as mean of data with three independent animals. *Error bars* represent means ± S.E. ($n = 3$). *, $p < 0.05$ using Student's *t* test. *C,* Western blots of two-dimensionally separated α- and β-tubulins of olfactory bulb samples. Note that β-tubulin of *pcd* olfactory bulb migrated to highly acidic region (*arrow*). α-Tubulin also shifted to the acidic region. *IB,* immunoblot. *D,* levels of TTLL1 and TTLL7 were examined by Western blot analysis of *pcd* and WT mouse brain regions. GAPDH was detected as loading control. An *arrowhead* points to the bands of TTLL1. *E,* quantitative analysis of TTL-like proteins levels in the *pcd* brain. Results are shown as mean of data with three independent animals. *Error bars* represent means ± S.E. ($n = 3$). No significant difference was detected with Student's *t* test ($p > 0.05$). *Panels A–E* used mice that were ~2 months old.

CCP1 and tubulin greatly extends this observation by demonstrating CCP1 enzyme activity at a molecular level.

Interestingly, our data show that purified CCP1 is capable of cleaving all Glu residues from the C terminus of α-tubulin to generate a new form of tubulin, delta3. When the levels of deTyr and delta2-tubulin were analyzed by Western blot, a significant decrease in both forms of tubulin was observed, indicating that CCP1 can cleave Glu from both deTyr and delta2 to generate delta3. When mass spectrometry analysis was performed, the peak corresponding to delta2-tubulin was increased after treatment of purified tubulin with CCP1. Considering that delta2 has the same mass as delta3 with one side chain Glu (2567.08 Da), and both forms represent the same peak in a spectrum, it is difficult to discriminate between them and conclude which one of these forms of tubulin contributes to the peak height. To resolve this question, tubulin was treated with purified CPO and then analyzed by mass spectrometry. CPO cleaves C-terminal Glu and polyE side chains, but it cannot remove a side chain Glu residue at the branch point (42). Thus, the 2567.09 peak in the CPO-treated sample represents

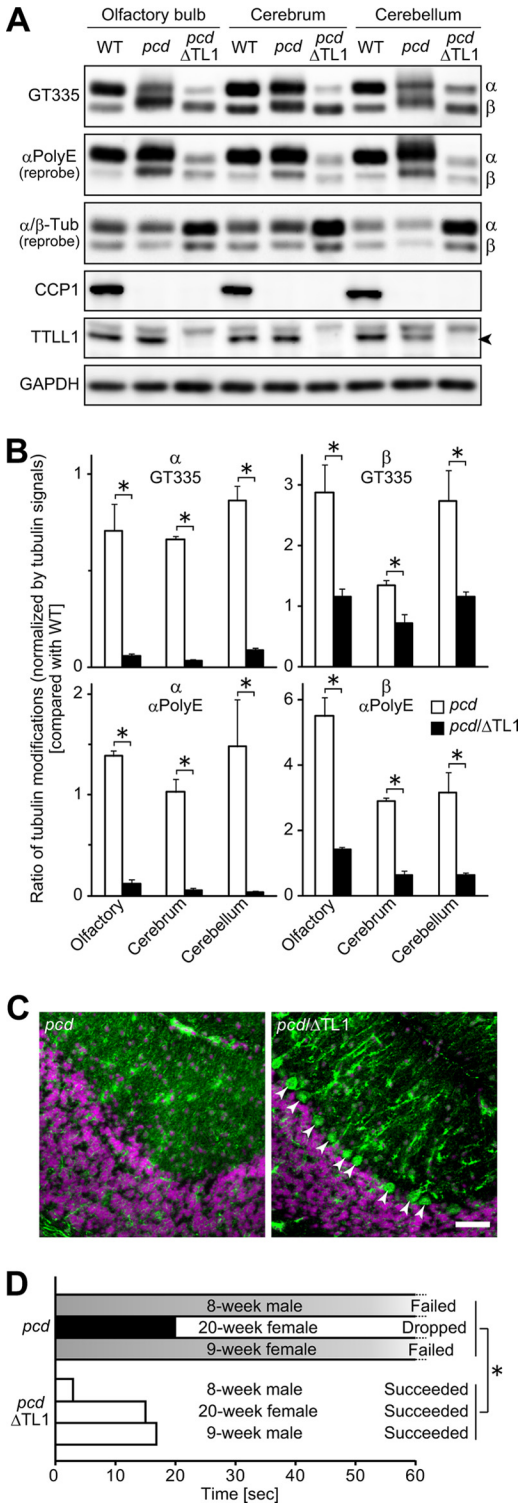

FIGURE 8. **Reduction of hyperpolyglutamylation of β-tubulin as well as α-tubulin in the *pcd*/ttll1KO brain.** *A,* representative Western blots for glutamylated and polyglutamylated α- and β-tubulins, CCP1, TTLL1, and GAPDH using ~2 month old mouse brain extracts. Signal intensities of polyglutamylated β-tubulin detected with αpolyE reached the same level as WT samples in the *pcd*/TTLL1-knock-out double mutant samples (*pcd*/ΔTL1). The band of β-tubulin detected with GT335 and αpolyE migrated to the same position as the WT band in the *pcd*/ΔTL1 samples. Glutamylated and polyglutamylated α-tubulin were grossly decreased in *pcd*/ΔTL1 samples. α- and β-tubulins were detected with independent antibodies, and so the relative intensities of the two forms do not appear identical. *Arrowhead* indicates the position of TTLL1. *B,* quantitative analysis of tubulin modifications in the *pcd* or *pcd*/ΔTL1 brain. Results are shown as mean of data with three independent animals. *Error bars* represent means ± S.E. ($n = 3$). *, $p < 0.05$ using Student's *t* test. *C,* immunohistochemical analysis of a cerebellum thin section. Neurons were labeled with anti-MAP1A. Nuclei were labeled with 4′,6-diamidino-2-phenylindole. In the *pcd*/ΔTL1 cerebellum, a number of Purkinje cells were observed (*arrowheads*). *Scale bar,* 50 μm. Three independent animals were examined for each genotype. *D,* behavioral test. Three animals of each genotype were analyzed. All *pcd*/ΔTL1 mice succeeded in the test within 20 s. In contrast, none of the *pcd* mice passed the test; they either failed to climb within 60 s (*failed*) or dropped from the cord (*dropped*). *, $p < 0.05$ using Student's *t* test with dropped data regarded as 60-s failure. Movies of representative mice are included in the supplemental information.

α-tubulin with no Glu at the C terminus but with a single Glu at the side chain (delta3 with a branch point Glu). These data indicate that CCP1 is capable of producing delta3-tubulin. To our knowledge, the delta3 form has not been previously described in the literature, although a previous study investigating PGs1-deficient mice found some α-tubulin migrated to a more basic position than delta2-tubulin in high resolution two-dimensional electrophoresis (47). It is possible that this form represented delta3-tubulin and that CCP1 can produce this form when TTLL1- and PGs1-containing enzymes are deficient. delta3-Tubulin may represent another potential modification, which may regulate microtubule dynamics.

In contrast to the results with purified brain tubulin, both overexpression of CCP1 in HEK293T cells and treatment of HEK293T microtubules with purified CCP1 caused an increase in the level of delta2-tubulin. The simple explanation for these seemingly contradictory results is that the major form of brain tubulin is delta2 (supplemental Fig. S3) (48). Thus, when CCP1 is incubated with brain tubulin, there is a large amount of substrate available for the enzyme to cleave to produce the delta3 form. Because HEK293T cells have very low levels of delta2 (Fig. 6, *A–C*), the major effect of CCP1 is the conversion of deTyr tubulin into delta2. Thus, considering the relative levels of each tubulin form, the results are not contradictory.

Our finding that levels of polyE α- and β-tubulin are increased in olfactory bulb and cerebellum of *pcd* mice supports the studies with cell culture and purified CCP1. The change in this tubulin modification in *pcd* mouse brain is not a consequence of elevated levels of glutamylation-performing enzymes because TTLL1 and TTLL7 proteins are not increased in *pcd* mouse brain. Rather, their levels are slightly decreased in *pcd* cerebellum (Fig. 7*C*), which could be explained by the loss of Purkinje cells and cerebellar atrophy. The levels of CCP mRNAs are also not altered in the brain of *pcd* mice. Thus, neither down-regulation of TTL-like proteins nor up-regulation of CCP mRNAs were observed in brain regions that do not undergo neurodegeneration in *pcd* mice, indicating that these other molecules do not compensate for the absence of CCP1 in mutant animals.

The finding that disruption of the *Ttll1* gene prevented hyperglutamylation of α-tubulin in *pcd* mouse brain is consistent with previous reports that the TTLL1-containing enzyme complex is involved in α-tubulin glutamylation in brain (25, 47). In contrast, β-tubulin glutamylation is thought to be performed by TTLL7 in neuronal tissues (26). Our finding that hyperglutamylation of β-tubulin in the *pcd* mouse brain was reduced by the knock-out of *Ttll1* shows that the control of glutamylation in mouse brain is more complex than previously

thought. TTLL1 is involved in the glutamylation of both α- and β-tubulin in tracheal ciliary axonemes (30). Furthermore, tubulin in ciliary or flagellar axonemes is reported to be hyperglutamylated in a steady state (49). Thus, it is possible that TTLL1 is involved in the hyperglutamylation of both α- and β-tubulin in mouse brain, which would account for our results.

The knock-out of *Ttll1* rescues *pcd* mice from Purkinje cell degeneration and ataxia even at 20 weeks of age (Fig. 8). These results support a recent report that virus-mediated RNAi against TTLL1 can reduce Purkinje cell death and ataxia in 5-week old *pcd* mice (29). Our data demonstrate the long term improvement of behavior of *pcd* mice and suggest the permanent cure of Purkinje cell loss and ataxia by the elimination of TTLL1 activity. However, the TTLL1 deletion did not rescue abnormal sperm morphology seen in *pcd* mice; there was deteriorated sperm morphology and motility due to a predominant effect of the TTLL1 deletion (data not shown).

Collectively, our *in vitro* and *in vivo* studies indicate that CCP1 is a functional cytosolic carboxypeptidase that removes Glu residues from the C terminus of α-tubulin and side chain Glu from both α- and β-tubulin. CCP1 has also been reported to remove glutamate residues from the C terminus of telokin (29). Furthermore, CCP5, a member of the CCP family, is also involved in the deglutamylation of both α- and β-tubulin (28). The number of CCPs involved in deglutamylation is smaller than that of TTL-like proteins involved in glutamylation: four CCPs for deglutamylation (28, 29) *versus* eight TTL-like proteins for glutamylation (25–27). A similar situation is observed in other post-translational modifications. For instance, the number of kinases is thought to be larger than the number of phosphatases.

The characterization of CCP1 activity reported here is consistent with the properties expected for an intracellular metallopeptidase, including a neutral pH optimum, maximal activity at low NaCl concentrations, and inhibition by metal chelation. Interestingly, no activation was observed with GTP, which was previously reported to activate another member of the CCP subfamily, CCP6 (3). Although CCP1 was originally described as an ATP/GTP-binding protein (1), there is no direct experimental evidence for this, and the purported ATP/GTP binding pocket is only distantly related to that of well studied ATP/GTP-binding proteins.

The role of CCP1 as a tubulin-processing enzyme is consistent with the broad cellular changes observed in the numerous previous studies on *pcd* mice. Cellular proteins and organelles need to be localized correctly in the cell to function properly, and their transport is tubulin-dependent. Microtubules play the role of the rails on which cargos are transported by motor proteins. Tubulin modifications are important for the affinity of motors and thus intracellular transport of the cellular cargoes. It was shown that the molecular motor kinesin binds preferentially to deTyr-tubulin to efficiently transport cargo (50, 51). Disruption of tubulin dynamics can cause mitochondrial dysfunction and lead to neurodegeneration (52). Recently, using *Caenorhabditis elegans* as an animal model, it was shown that tubulin deglutamylation by CCP1 regulates localization and activity of molecular motors in cilia (53). Changes in tubulin processing can potentially explain the myriad defects found in *pcd* mice, including abnormal accumulation of polysomes (9), altered transcription and DNA repair (10, 11), endoplasmic reticulum stress (12), formation of axonal spheroids (13), mitochondrial dysfunction (14), elevated autophagy (15), and abnormal dendritic development (16). However, there are other cytosolic proteins that require polyglutamylation and/or deglutamylation modifications (29, 54). Thus, it is possible that changes in other CCP1 substrates could contribute to the phenotype of the *pcd* mouse. It remains to be determined how a defect in processing of tubulin and/or other potential CCP1 substrates contributes to some of the previously noted changes, such as the large increase in cytosolic peptides found in *pcd* mouse brain regions (15). Because the vast majority of these peptides had C-terminal hydrophobic or basic residues, and not acidic residues, it is unlikely that CCP1 plays a direct role in peptide degradation, and so the effect is likely to be indirect, either through tubulin or another protein cleaved by CCP1.

Acknowledgments—Mass spectrometry for the analysis of peptides in HEK293T cells was performed in the laboratory of Prof. Fabio Gozzo, Universidade de Campinas, Brazil, by Leandro M. Castro and was supported by grants from São Paulo State Research Foundation, Financiadora de Estudos e Projetos, and Brazilian National Research Council. Antibodies to tubulin were provided by Prof. Martin Gorovsky (University of Rochester, Rochester, NY) and by Prof. Carsten Janke (Université Montpellier, France).

REFERENCES

1. Harris, A., Morgan, J. I., Pecot, M., Soumare, A., Osborne, A., and Soares, H. D. (2000) Regenerating motor neurons express Nna1, a novel ATP/GTP-binding protein related to zinc carboxypeptidases. *Mol. Cell. Neurosci.* **16,** 578–596
2. Kalinina, E., Biswas, R., Berezniuk, I., Hermoso, A., Aviles, F. X., and Fricker, L. D. (2007) A novel subfamily of mouse cytosolic carboxypeptidases. *FASEB J.* **21,** 836–850
3. Rodriguez de la Vega, M., Sevilla, R. G., Hermoso, A., Lorenzo, J., Tanco, S., Diez, A., Fricker, L. D., Bautista, J. M., and Avilés, F. X. (2007) Nna1-like proteins are active metallocarboxypeptidases of a new and diverse M14 subfamily. *FASEB J.* **21,** 851–865
4. Fernandez-Gonzalez, A., La Spada, A. R., Treadaway, J., Higdon, J. C., Harris, B. S., Sidman, R. L., Morgan, J. I., and Zuo, J. (2002) Purkinje cell degeneration (*pcd*) phenotypes caused by mutations in the axotomy-induced gene, *Nna1*. *Science* **295,** 1904–1906
5. Mullen, R. J., Eicher, E. M., and Sidman, R. L. (1976) Purkinje cell degeneration, a new neurological mutation in the mouse. *Proc. Natl. Acad. Sci. U.S.A.* **73,** 208–212
6. Wang, T., and Morgan, J. I. (2007) The Purkinje cell degeneration (*pcd*) mouse. An unexpected molecular link between neuronal degeneration and regeneration. *Brain Res.* **1140,** 26–40
7. Wang, T., Parris, J., Li, L., and Morgan, J. I. (2006) The carboxypeptidase-like substrate-binding site in Nna1 is essential for the rescue of the Purkinje cell degeneration (*pcd*) phenotype. *Mol. Cell. Neurosci.* **33,** 200–213
8. Chakrabarti, L., Eng, J., Martinez, R. A., Jackson, S., Huang, J., Possin, D. E., Sopher, B. L., and La Spada, A. R. (2008) The zinc-binding domain of Nna1 is required to prevent retinal photoreceptor loss and cerebellar ataxia in Purkinje cell degeneration (*pcd*) mice. *Vision Res.* **48,** 1999–2005
9. Landis, S. C., and Mullen, R. J. (1978) The development and degeneration of Purkinje cells in *pcd* mutant mice. *J. Comp. Neurol.* **177,** 125–143
10. Valero, J., Berciano, M. T., Weruaga, E., Lafarga, M., and Alonso, J. R. (2006) Pre-neurodegeneration of mitral cells in the *pcd* mutant mouse is associated with DNA damage, transcriptional repression, and reorganization of nuclear speckles and Cajal bodies. *Mol. Cell. Neurosci.* **33,** 283–295
11. Baltanás, F. C., Casafont, I., Lafarga, V., Weruaga, E., Alonso, J. R., Ber-

ciano, M. T., and Lafarga, M. (2011) Purkinje cell degeneration in *pcd* mice reveals large scale chromatin reorganization and gene silencing linked to defective DNA repair. *J. Biol. Chem.* **286,** 28287–28302
12. Kyuhou, S., Kato, N., and Gemba, H. (2006) Emergence of endoplasmic reticulum stress and activated microglia in Purkinje cell degeneration mice. *Neurosci. Lett.* **396,** 91–96
13. Bäurle, J., and Grüsser-Cornehls, U. (1994) Axonal torpedoes in cerebellar Purkinje cells of two normal mouse strains during aging. *Acta Neuropathol.* **88,** 237–245
14. Chakrabarti, L., Zahra, R., Jackson, S. M., Kazemi-Esfarjani, P., Sopher, B. L., Mason, A. G., Toneff, T., Ryu, S., Shaffer, S., Kansy, J. W., Eng, J., Merrihew, G., MacCoss, M. J., Murphy, A., Goodlett, D. R., Hook, V., Bennett, C. L., Pallanck, L. J., and La Spada, A. R. (2010) Mitochondrial dysfunction in NnaD mutant flies and Purkinje cell degeneration mice reveals a role for Nna proteins in neuronal bioenergetics. *Neuron* **66,** 835–847
15. Berezniuk, I., Sironi, J., Callaway, M. B., Castro, L. M., Hirata, I. Y., Ferro, E. S., and Fricker, L. D. (2010) CCP1/Nna1 functions in protein turnover in mouse brain. Implications for cell death in Purkinje cell degeneration mice. *FASEB J.* **24,** 1813–1823
16. Li, J., Gu, X., Ma, Y., Calicchio, M. L., Kong, D., Teng, Y. D., Yu, L., Crain, A. M., Vartanian, T. K., Pasqualini, R., Arap, W., Libermann, T. A., Snyder, E. Y., and Sidman, R. L. (2010) Nna1 mediates Purkinje cell dendritic development via lysyl oxidase propeptide and NF-κB signaling. *Neuron* **68,** 45–60
17. Berezniuk, I., and Fricker, L. D. (2010) A defect in cytosolic carboxypeptidase 1 (Nna1) causes autophagy in Purkinje cell degeneration mouse brain. *Autophagy* **6,** 558–559
18. Ikegami, K., and Setou, M. (2010) Unique post-translational modifications in specialized microtubule architecture. *Cell Struct. Funct.* **35,** 15–22
19. Wloga, D., and Gaertig, J. (2010) Post-translational modifications of microtubules. *J. Cell Sci.* **123,** 3447–3455
20. Janke, C., and Bulinski, J. C. (2011) Post-translational regulation of the microtubule cytoskeleton. Mechanisms and functions. *Nat. Rev. Mol. Cell Biol.* **12,** 773–786
21. Argaraña, C. E., Barra, H. S., and Caputto, R. (1978) Release of [^{14}C]tyrosine from tubulinyl-[^{14}C]tyrosine by brain extract. Separation of a carboxypeptidase from tubulin-tyrosine ligase. *Mol. Cell. Biochem.* **19,** 17–21
22. Raybin, D., and Flavin, M. (1977) Enzyme that specifically adds tyrosine to the α chain of tubulin. *Biochemistry* **16,** 2189–2194
23. Paturle-Lafanechère, L., Eddé, B., Denoulet, P., Van Dorsselaer, A., Mazarguil, H., Le Caer, J. P., Wehland, J., and Job, D. (1991) Characterization of a major brain tubulin variant that cannot be tyrosinated. *Biochemistry* **30,** 10523–10528
24. Eddé, B., Rossier, J., Le Caer, J. P., Desbruyères, E., Gros, F., and Denoulet, P. (1990) Post-translational glutamylation of α-tubulin. *Science* **247,** 83–85
25. Janke, C., Rogowski, K., Wloga, D., Regnard, C., Kajava, A. V., Strub, J. M., Temurak, N., van Dijk, J., Boucher, D., van Dorsselaer, A., Suryavanshi, S., Gaertig, J., and Eddé, B. (2005) Tubulin polyglutamylase enzymes are members of the TTL domain protein family. *Science* **308,** 1758–1762
26. Ikegami, K., Mukai, M., Tsuchida, J., Heier, R. L., Macgregor, G. R., and Setou, M. (2006) TTLL7 is a mammalian β-tubulin polyglutamylase required for growth of MAP2-positive neurites. *J. Biol. Chem.* **281,** 30707–30716
27. van Dijk, J., Rogowski, K., Miro, J., Lacroix, B., Eddé, B., and Janke, C. (2007) A targeted multienzyme mechanism for selective microtubule polyglutamylation. *Mol. Cell.* **26,** 437–448
28. Kimura, Y., Kurabe, N., Ikegami, K., Tsutsumi, K., Konishi, Y., Kaplan, O. I., Kunitomo, H., Iino, Y., Blacque, O. E., and Setou, M. (2010) Identification of tubulin deglutamylase among *Caenorhabditis elegans* and mammalian cytosolic carboxypeptidases (CCPs). *J. Biol. Chem.* **285,** 22936–22941
29. Rogowski, K., van Dijk, J., Magiera, M. M., Bosc, C., Deloulme, J. C., Bosson, A., Peris, L., Gold, N. D., Lacroix, B., Grau, M. B., Bec, N., Larroque, C., Desagher, S., Holzer, M., Andrieux, A., Moutin, M. J., and Janke, C. (2010) A family of protein-deglutamylating enzymes associated with neurodegeneration. *Cell* **143,** 564–578
30. Ikegami, K., Sato, S., Nakamura, K., Ostrowski, L. E., and Setou, M. (2010) Tubulin polyglutamylation is essential for airway ciliary function through the regulation of beating asymmetry. *Proc. Natl. Acad. Sci. U.S.A.* **107,** 10490–10495
31. Morano, C., Zhang, X., and Fricker, L. D. (2008) Multiple isotopic labels for quantitative mass spectrometry. *Anal. Chem.* **80,** 9298–9309
32. Berti, D. A., Morano, C., Russo, L. C., Castro, L. M., Cunha, F. M., Zhang, X., Sironi, J., Klitzke, C. F., Ferro, E. S., and Fricker, L. D. (2009) Analysis of intracellular substrates and products of thimet oligopeptidase in human embryonic kidney 293 cells. *J. Biol. Chem.* **284,** 14105–14116
33. Gelman, J. S., Sironi, J., Castro, L. M., Ferro, E. S., and Fricker, L. D. (2010) Hemopressins and other hemoglobin-derived peptides in mouse brain. Comparison between brain, blood, and heart peptidome and regulation in Cpefat/fat mice. *J. Neurochem.* **113,** 871–880
34. Wardman, J., and Fricker, L. D. (2011) Quantitative peptidomics of mice lacking peptide-processing enzymes. *Methods Mol. Biol.* **768,** 307–323
35. Wolff, A., de Néchaud, B., Chillet, D., Mazarguil, H., Desbruyères, E., Audebert, S., Eddé, B., Gros, F., and Denoulet, P. (1992) Distribution of glutamylated α- and β-tubulin in mouse tissues using a specific monoclonal antibody, GT335. *Eur. J. Cell Biol.* **59,** 425–432
36. Wei, S., Segura, S., Vendrell, J., Aviles, F. X., Lanoue, E., Day, R., Feng, Y., and Fricker, L. D. (2002) Identification and characterization of three members of the human metallocarboxypeptidase gene family. *J. Biol. Chem.* **277,** 14954–14964
37. Vassal, E., Barette, C., Fonrose, X., Dupont, R., Sans-Soleilhac, E., and Lafanechère, L. (2006) Miniaturization and validation of a sensitive multiparametric cell-based assay for the concomitant detection of microtubule-destabilizing and microtubule-stabilizing agents. *J. Biomol. Screen.* **11,** 377–389
38. Fricker, L. D., and Snyder, S. H. (1982) Enkephalin convertase. Purification and characterization of a specific enkephalin-synthesizing carboxypeptidase localized to adrenal chromaffin granules. *Proc. Natl. Acad. Sci. U.S.A.* **79,** 3886–3890
39. Song, L., and Fricker, L. D. (1995) Purification and characterization of carboxypeptidase D, a novel carboxypeptidase E-like enzyme, from bovine pituitary. *J. Biol. Chem.* **270,** 25007–25013
40. Nalamachu, S. R., Song, L., and Fricker, L. D. (1994) Regulation of carboxypeptidase E. Effect of Ca^{2+} on enzyme activity and stability. *J. Biol. Chem.* **269,** 11192–11195
41. Fernandez, D., Boix, E., Pallares, I., Aviles, F. X., and Vendrell, J. (2011) *Enzyme Res.* **2011,** 128676
42. Lyons, P. J., and Fricker, L. D. (2011) Carboxypeptidase O is a glycosylphosphatidylinositol-anchored intestinal peptidase with acidic amino acid specificity. *J. Biol. Chem.* **286,** 39023–39032
43. Schulze, E., Asai, D. J., Bulinski, J. C., and Kirschner, M. (1987) Post-translational modification and microtubule stability. *J. Cell Biol.* **105,** 2167–2177
44. Schiff, P. B., and Horwitz, S. B. (1980) Taxol stabilizes microtubules in mouse fibroblast cells. *Proc. Natl. Acad. Sci. U.S.A.* **77,** 1561–1565
45. Shang, Y., Li, B., and Gorovsky, M. A. (2002) *Tetrahymena thermophila* contains a conventional γ-tubulin that is differentially required for the maintenance of different microtubule-organizing centers. *J. Cell Biol.* **158,** 1195–1206
46. Wloga, D., Rogowski, K., Sharma, N., Van Dijk, J., Janke, C., Eddé, B., Bré, M. H., Levilliers, N., Redeker, V., Duan, J., Gorovsky, M. A., Jerka-Dziadosz, M., and Gaertig, J. (2008) Glutamylation on α-tubulin is not essential but affects the assembly and functions of a subset of microtubules in *Tetrahymena thermophila*. *Eukaryot. Cell* **7,** 1362–1372
47. Ikegami, K., Heier, R. L., Taruishi, M., Takagi, H., Mukai, M., Shimma, S., Taira, S., Hatanaka, K., Morone, N., Yao, I., Campbell, P. K., Yuasa, S., Janke, C., Macgregor, G. R., and Setou, M. (2007) Loss of α-tubulin polyglutamylation in ROSA22 mice is associated with abnormal targeting of KIF1A and modulated synaptic function. *Proc. Natl. Acad. Sci. U.S.A.* **104,** 3213–3218
48. Paturle-Lafanechere, L., Manier, M., Trigault, N., Pirollet, F., Mazarguil, H., and Job, D. (1994) Accumulation of delta2-tubulin, a major tubulin variant that cannot be tyrosinated, in neuronal tissues and in stable mi-

crotubule assemblies. *J. Cell Sci.* **107** 1529–1543
49. Million, K., Larcher, J., Laoukili, J., Bourguignon, D., Marano, F., and Tournier, F. (1999) Polyglutamylation and polyglycylation of α- and β-tubulins during *in vitro* ciliated cell differentiation of human respiratory epithelial cells. *J. Cell Sci.* **112** 4357–4366
50. Kreitzer, G., Liao, G., and Gundersen, G. G. (1999) Detyrosination of tubulin regulates the interaction of intermediate filaments with microtubules *in vivo* via a kinesin-dependent mechanism. *Mol. Biol. Cell* **10,** 1105–1118
51. Dunn, S., Morrison, E. E., Liverpool, T. B., Molina-París, C., Cross, R. A., Alonso, M. C., and Peckham, M. (2008) Differential trafficking of Kif5c on tyrosinated and detyrosinated microtubules in live cells. *J. Cell Sci.* **121,** 1085–1095
52. Cartelli, D., Ronchi, C., Maggioni, M. G., Rodighiero, S., Giavini, E., and Cappelletti, G. (2010) Microtubule dysfunction precedes transport impairment and mitochondria damage in MPP^+-induced neurodegeneration. *J. Neurochem.* **115,** 247–258
53. O'Hagan, R., Piasecki, B. P., Silva, M., Phirke, P., Nguyen, K. C., Hall, D. H., Swoboda, P., and Barr, M. M. (2011) The tubulin deglutamylase CCPP-1 regulates the function and stability of sensory cilia in *C. elegans*. *Curr. Biol.* **21,** 1685–1694
54. van Dijk, J., Miro, J., Strub, J. M., Lacroix, B., van Dorsselaer, A., Edde, B., and Janke, C. (2008) Polyglutamylation is a post-translational modification with a broad range of substrates. *J. Biol. Chem.* **283,** 3915–3922